Inflammatory Bowel Diseases, 2026, 32, 1219–1234
https://doi.org/10.1093/ibd/izag066
Published: May 14, 2026
Original Research Article - Leading Off

CB_2R promotes T cell gut homing and exacerbates ileitis in a murine Crohn's model

Robert S. Leddy, PhD[1,2,†], Cinthia L. Hudachek, PhD[3,†], Hannah M. Phelan, BSc[1,2], Carol M. Aherne, PhD[2,4], Julián Romero, PhD[5], Cecilia J. Hillard, PhD[6], Zhiran Wang, PhD[7], Günther Eissner, PhD[7], Paul Jedlicka, MD[8], Colm B. Collins, PhD[*,1,2]

[1]School of Biomolecular and Biomedical Science, University College Dublin, Dublin, Ireland
[2]UCD Conway Institute of Biomolecular and Biomedical Research, University College Dublin, Dublin, Ireland
[3]Section of Gastroenterology, Hepatology and Nutrition, Department of Pediatrics, University of Colorado Anschutz Medical Campus, Aurora, CO, United States
[4]School of Medicine, University College Dublin, Dublin, Ireland
[5]Faculty of Experimental Sciences, Universidad Francisco de Vitoria, Pozuelo de Alarcón, Spain
[6]Department of Pharmacology and Toxicology, Neuroscience Research Center, Medical College of Wisconsin, Milwaukee, WI, United States
[7]Systems Biology Ireland, School of Medicine, University College Dublin, Dublin, Ireland
[8]Department of Pathology, University of Colorado Anschutz Medical Campus, Aurora, CO, United States

[†]Co-first authors.
[*]Corresponding author: Colm B. Collins, PhD, UCD Conway Institute, University College Dublin, Belfield, Dublin 4, D04 V1W8, Ireland (colm.collins@ucd.ie).

Abstract

Leukocyte trafficking is a critical step in the development of chronic intestinal diseases such as Crohn's disease. While strategies that block gut homing have yielded partial success, this disease remains uncurable leaving an unmet clinical need. This is the first paper to describe a role for cannabinoid receptor 2 (CB_2R) signaling in promoting retinoic acid-mediated induction of the gut homing associated integrin heterodimer $\alpha4\beta7$. Using in vitro and in vivo models, we characterized the effects of pharmacological CB_2R agonists and inverse agonists on T cell homing receptor expression and transmigration across gut-associated endothelial barriers. This extracellular signal-regulated kinase–dependent process coincides with increased T cell adherence in response to CB_2R agonism with JWH-133. These effects were reversed with an inverse agonist GP-1a in a CB_2R dependent manner. Selective deletion of CB_2R using CRISPR in vitro or $CD4^{Cre/+}$ floxed mice in vivo resulted in impaired endothelial cell adherence and decreased diapedesis into the ileal lamina propria. T cell–specific deletion of *CNR2*, the gene encoding CB_2R, attenuated chronic murine ileitis characterized by decreased naïve T cell infiltration and loss of tissue architecture in 20-week-old $TNF^{\Delta ARE/+}$ mice. This study supports further therapeutic development of CB_2R-targeting drugs for the treatment of inflammatory bowel disease.

Key words: chronic ileitis, cannabinoids, T cell adherence, CB_2R.

Received: December 15, 2025. **Accepted:** March 23, 2026

Key Messages

- Cannabis use is increasingly popular among people living with IBD due to its ability to reduce bowel frequency, suppress perception of visceral pain and reverse loss of appetite, however, chronic use is linked to increased surgical risk.
- This paper uses pharmacological and cell-specific genetic deletion to demonstrate an unappreciated role for the cannabinoid receptor 2 (CB_2R) in driving gut homing via increased $\alpha4\beta7$ expression on human and murine T cells.
- $CD4^+$ T cell–specific CB_2R deletion attenuates chronic murine ileitis, supporting further therapeutic development of CB_2R-targeting ligands, while this information may also be invaluable for patients considering cannabis use for symptomatic relief.

Introduction

Inflammatory bowel disease (IBD), encompassing Crohn's disease (CD) and ulcerative colitis (UC), is a chronic, relapsing inflammatory disorder of the gastrointestinal tract characterized by dysregulated immune responses and impaired intestinal homeostasis. People with IBD may experience severe chronic visceral pain, which is challenging to manage, in part because of the negative impact of opioid analgesics on digestive function and epithelial repair.[1,2]

Cannabis is seen by patients as a potential means to alleviate chronic pain and motility dysfunction associated with IBD.[3] The endocannabinoid system (ECS) signals primarily via two G protein–coupled receptors, cannabinoid receptor 1 (CB_1R) and CB_2R. These are G protein–coupled receptors that primarily couple to $G_{i/o}$ proteins,[4] leading to inhibition of adenylate cyclase, decreased cyclic adenosine monophosphate levels, and modulation of downstream signaling pathways such as mitogen-activated protein kinases (MAPKs) (extracellular signal-regulated kinase 1/2 [ERK1/2], p38, JNK).[5–7] These pathways regulate diverse cellular processes including cytokine production, cell migration, proliferation, and apoptosis. This is further regulated by the distinct expression patterns and functions of these receptors. CB_1R, abundant in the central nervous system, regulates neurotransmission, including the psychoactive effects synonymous with cannabis products,[8] while also regulating intestinal secretion and motility via its expression on enteric neurons.[9] Conversely, CB_2R, while certainly induced in the brain during inflammation,[10,11] is predominantly expressed in immune tissues (spleen, lymph nodes, bone marrow) and hematopoietic cells, including T cells, macrophages, and neutrophils, at levels up to 100-fold higher than CB_1R. This immune-focused distribution identifies CB_2R as a potential regulator of inflammation and, lacking psychoactive effects, highlights its appeal as a therapeutic target for treating inflammatory diseases.

In the context of intestinal inflammation, both animal models and human studies have demonstrated upregulation of CB_2R and increased levels of ECS ligands in the gut.[12,13] For instance, CB_2R expression is markedly increased on infiltrating immune cells in experimental colitis models[14,15] and in the inflamed mucosa of IBD patients.[12,16–18] Similarly, elevated levels of ECS ligands anandamide and 2-arachidonoylglycerol have been observed in the intestinal tissues and plasma of individuals with active IBD, correlating with disease severity.[19–21]

Furthermore, selective CB_2R agonist APD371 has proven effective in clinical trials at decreasing visceral pain.[22] However, clinical trials with phytocannabinoids consistently fail to demonstrate efficacy in disease modification. A randomized study of CD patients revealed symptomatic improvement without achieving increased clinical remission, while a trial in UC showed no improvement in remission rates between cannabis and placebo groups despite quality-of-life benefits.[23,24] A 2021 trial further corroborated the dissociation between subjective relief and objective inflammatory markers,[25] a finding reinforced by a Cochrane meta-analysis highlighting insufficient evidence for cannabis in IBD remission induction or maintenance.[26] Of greater concern is that prolonged cannabis use (>6 months) correlates with worsened CD outcomes, including a 5-fold increase in surgical risk,[27] underscoring unresolved controversies regarding its therapeutic potential.

CB_2R also appears to play a role in regulating immune cell trafficking, a process critical for maintaining intestinal immune surveillance and homeostasis. In the experimental autoimmune encephalomyelitis mouse model of multiple sclerosis, CB_2R activation has been demonstrated to have protective effects by reducing $CD4^+$ T cell infiltration and microglial activation, leading to improved disease outcomes.[28] Conversely, CB_2R-deficient mice exhibited worse disease outcomes, including increased $CD4^+$ T cell infiltration of the brain, highlighting the receptor's importance in this regard.[28] Similarly, chronic administration of tetrahydrocannabinol, an active compound found in cannabis, to simian immunodeficiency virus–infected male rhesus monkeys increased intestinal integrin $\alpha4\beta7^+CD4^+$ T cells, $CD8^+$ T cells, and central memory T cells and the significant increase in the expression of proinflammatory cytokines within the gut.[29] Our lab has previously demonstrated that inverse agonism of CB_2R attenuates inflammation in a preclinical Crohn's model with a concomitant decrease in infiltrating T cells in the murine ileal lamina propria (LP).[12] Dysregulation of leukocyte trafficking contributes to the chronic inflammation characteristic of IBD and may contribute to cannabinoid-mediated exacerbation of chronic disease. Gut-specific homing is primarily driven by $\alpha4\beta7$ expression on circulating T cells interacting with mucosal addressin cell adhesion molecule 1 (MAdCAM-1) on endothelial cells.[30]

Retinoic acid (RA) induces stable $\alpha4\beta7$ expression on $CD4^+$ T cells via epigenetic regulation, ensuring that even when these cells migrate away from the required RA signal, they retain the imprinted gut homing "zip-code" resulting in long-lasting gut homing T cells. During priming, RA blocks the methylation of specific CpG sites upstream of the *ITGA4* promoter in mice and humans, leading to the stable expression of $\alpha4\beta7$ but not $\alpha4\beta1$.[31] Interestingly, CB_2R activation has been shown to mimic these epigenetic events induced by RA via triggering the same histone modifications,[32] meaning it may be possible that receptor activation could promote gut homing properties. Alternatively, CB_2R may regulate integrin expression via MAPK signaling. CB_2R's role in MAPK signaling was first identified by Bouaboula et al,[33] who showed that CB_2R activation leads to ERK1/2 phosphorylation. Subsequent studies have found CB_2R

activation to trigger p38 MAPK in lymphoma cells and induce the activation of ERK1/2 and JNK MAPK in microglial cells.[34] CB_2R activation also drives phosphorylation of ERK1/2 in T cells[35] and epithelial cells,[36] leading to proinflammatory cytokine release. The goal of this study is therefore to understand the impact of CB_2R activation on $CD4^+$ T cell trafficking including downstream signaling and integrin regulation. By extension, we aim to understand the contribution of CB_2R activation to chronic intestinal disease.

Methods

Cellular adhesion assays

Jurkat E6-1 human T lymphocytic leukemia cell line (ATCC) was maintained at 37 °C (95% O_2/5% CO_2) in RPMI 1640 containing L-glutamine (Thermo Fisher Scientific; #61870-010) supplemented with 1% penicillin-streptomycin (Thermo Fisher Scientific; #15140122) and 10% fetal bovine serum (Merck; #F9665). Jurkat T cells (2.5×10^6 cells/mL) were cultured in RPMI 1640 and treated in triplicate with 1 μM RA (Merck; Cat No. R2625) ± 1 μM JWH-133 (CB_2R agonist, Tocris Bioscience; #1343/10), or 10 μM GP-1a (CB_2R inverse agonist, Tocris Bioscience; #2764/10) for 48 hours; vehicle controls received media alone. Cells were counted, resuspended in Hanks' Buffered Salt Solution (Thermo Fisher Scientific; #14065-056) + 0.5 mM Manganese Chloride ($MnCl_2$, Sigma-Aldrich; #M8054-100G), and added to 24-well plates precoated with recombinant MAdCAM-1 (3 ng/μL; Bio-Techne; #6056-MC). After 30 minutes at 37 °C, nonadherent cells were removed and adhered cells were trypsinized (200 μL, 2-3 minutes, room temperature; Thermo Fisher Scientific; #25300-054) and recounted. Adhesion percentage was calculated as (adhered cells/total cells) × 100.

MAdCAM-1–dependent cellular adhesion assay

Jurkat T cells (2.5×10^6 cells/mL in RPMI 1640) were treated in triplicate with 1 μM RA ± 1 μM JWH-133 or 10 μM GP-1a for 48 hours; vehicle controls received media alone. Concurrently, HEK293T cells (ATCC) stably expressing MAdCAM-1 (1×10^6 cells/well in Dulbecco's Modified Eagle Medium (DMEM, Lonza Scientific; #12707F) supplemented with 10% fetal bovine serum, 1% penicillin-streptomycin, and 1.24% L-glutamine (Thermo Fisher Scientific; #25030-024)) were seeded to achieve > 90% confluency after 48 hours. The Jurkat cells were harvested, stained with 5 μM CFDA (Thermo Fisher Scientific; V12883) in phosphate-buffered saline (PBS, Thermo Fisher Scientific; #1282-1680) (15 minutes, 37 °C), and washed. CFDA-labeled Jurkat cells (1 mL) were added to MAdCAM-1–expressing HEK293T monolayers and cocultured for 30 minutes at 37 °C. Nonadherent cells were aspirated, and adhered Jurkat cells were detached with 200 μL trypsin (2-3 minutes, room temperature). Adherent cells were quantified via fluorescence microscopy (Olympus CKX41/EP50) and expressed as before.

For cellular adhesion assays under shear stress, m-Slide I Luer 3D slides (Ibidi; #87176) and supplemented DMEM were degassed overnight at 37 °C. On the following day, slides were coated with 3.3 μg/mL Rat Collagen I (Cultrex; #3440-100-01) in PBS for 2 hours at 37 °C, followed by application of a collagen gel matrix composed of 60% collagen, 10% 10× PBS (Thermo Fisher Scientific; #70013-016), 14% $NaHCO_3$, 16% DMEM, and 46% deionized water, with polymerization for 2 hours at 37 °C. Human umbilical vein endothelial cells (HUVECs; ATCC) were maintained in supplemented DMEM, labeled in serum-free DMEM at 2×10^6 cells/mL with 1 μM CellTracker Orange CMTMR (Invitrogen; #C2927) for 30 minutes at 37 °C, washed, and seeded into the slides at 1.6×10^6 cells/mL, then cultured overnight. Wild-type (WT) and $CNR2^{-/-}$ Jurkat T cells were resuspended at 3×10^6 cells/mL and treated with 1 μM JWH-133 in T25 flasks (Greiner; #C6356) for 24 hours at 37 °C. The following day, Jurkat cells were stained with 0.33 μM CellTracker Green CMFDA (Invitrogen; #C7025) for 30 minutes at 37 °C, washed, and resuspended in prewarmed, degassed, phenol red–free RPMI (Thermo Fisher Scientific; #11835063) at 0.1×10^6 cells/mL. Cell suspensions were loaded into syringe pumps and perfused through the HUVEC-coated slides, which had been preconditioned with phenol red–free RPMI, at a shear stress of 0.4 dyn/cm^2 for 18 hours (flow rate calculated per manufacturer's instructions). After perfusion, slides were washed with PBS, fixed with 4% paraformaldehyde (PFA, Thermo Fisher Scientific; #J19943.K2) for 30 minutes at room temperature, and washed again prior to imaging on an Olympus FV1000 confocal microscope. Adhered Jurkat cells were quantified from three images per chamber, with the mean value used for analysis.

Jurkat T cell gene expression analysis

Jurkat T cells plated at 2.5×10^6 cells/mL were treated for 48 hours with RA (1 μM) ± CB_2R agonist JWH-133 (1 μM) or CB_2R inverse agonist GP-1a (10 μM)[37]; vehicle controls received media alone. Ligands were tested in luciferase and polymerase chain reaction (PCR) assays at both 24 hours and 48 hours at 0.1 to 10 μM to identify optimal conditions for further analysis (Figure S1). Cells were harvested and washed in PBS, and total RNA was extracted using the RNeasy Mini kit (Qiagen; #74106) according to the manufacturer's instructions. Eluted RNA samples were then sent for transcriptomic profiling sequencing by BGI Genomics, with an RNA integrity number of ≥ 6.5 used as a RNA quality cutoff for inclusion in analysis. Raw sequencing data were converted to FASTQ file format using Illumina and uploaded to Galaxy, before quality control of reads was done using the Cutadapt pipeline. The cleaned reads were then mapped to a reference genome using STAR and checked using the Integrative Genomics Viewer. From the mapped sequences, the number of reads per annotated genes were counted using the featurecounts package. The DESeq2 package was then used on the read counts to normalize and extract differentially expressed genes between treatment groups. Functional enrichment and pathway analysis of the differentially expressed genes was performed using the Fast Gene Set Enrichment Analysis (fgsea) package to extract any interesting gene ontologies. The full analysis dataset is available at https://www.ncbi.nlm.nih.gov/bioproject/PRJNA1301825. For expression analysis, isolated RNA was transcribed using a high-capacity cDNA Reverse Transcription Kit (Applied Biosystems; #4368814). Relative quantification of messenger RNA (mRNA) expression was performed using TaqMan Gene

Expression Assays and the QuantStudio 12K Flex Real-Time PCR System. Real-time PCR assays for *ITGB7* (Thermo Fisher Scientific; Hs01565750_m1), *ITGA4* (Thermo Fisher Scientific; Hs00168433_m1), *ITGAE* (Thermo Fisher Scientific; Hs01025372_m1), *ITGB1* (Thermo Fisher Scientific; Hs01127536_m1), and *CNR2* (Thermo Fisher Scientific; Hs05019229_s1) were carried out, with ribosomal 18s (Applied Biosciences; Cat No. 4319413E) as an endogenous control.

Biological network analysis

Biological network, functional, and pathway analyses were performed using Ingenuity Pathway Analysis (IPA) (Ingenuity Systems). For canonical pathway and network analyses, gene lists containing up- and downregulated transcripts (with corresponding log2 fold change and adjusted *P* values) from RNA sequencing of JWH-133 or GP-1a–treated cells were imported into IPA. No stringent filtering criteria were applied, enabling comprehensive identification of transcriptionally regulated pathways and networks. IPA determined the degree of pathway regulation based on log2 fold change and –log10(adjusted *P* value) for each gene.

Dual luciferase promoter reporter assays

Jurkat T cells were seeded in 24-well plates (2.5×10^5 cells/well) and transfected with 1 µg DNA/well using Lipofectamine LTX with PLUS Reagent (Thermo Fisher Scientific; #A12621). Constructs included full length or truncated *ITGB7* sequences cloned into pGL4 vectors (GenScript), cotransfected with *Renilla* luciferase plasmid (9:1 ratio). Cells were treated 24 hours post-transfection as indicated. Lysates resuspended in 100 µL Passive Lysis Buffer (Promega; #E1960) were analyzed for firefly and *Renilla* luciferase activities using a ClarioStar PLUS plate reader (BMG LabTech). Normalized relative luciferase units were calculated and visualized in GraphPad Prism 10 (GraphPad Software).

Mice

$TNF^{\Delta ARE/+}$ mice (B6.129S-Tnftm2GKI/Jarn; MGI: 3720980) were previously generated by backcrossing heterozygous $TNF^{\Delta ARE/+}$ mice to C57BL/6J. $CD4^{Cre}$ and $RAG1^{-/-}$ mice (Jackson Laboratory) were bred in-house and crossed with $CB_2R^{Fl/Fl}$ mice (provided by C.J. Hillard and J. Romero Paredes)[38] to generate $CB_2R^{Fl/Fl}CD4^{Cre}TNF^{\Delta ARE/+}$ triple transgenics; Cre-negative littermates served as control mice. Mice of both sexes were used interchangeably in these studies except for adoptive transfer studies in which female donor T cells were not injected into male $RAG1^{-/-}$ recipients to avoid graft-vs-host disease.

Flow cytometry and staining

For cytokine profiling, splenocytes, mesenteric lymphocytes, and LP mononuclear cells were stimulated for 3 hours at 37 °C with 50 ng/mL PMA (Sigma-Aldrich; #P8139), 1 µg/mL ionomycin (Sigma-Aldrich; #I0634), and 10 µg/mL brefeldin A (Sigma-Aldrich; #B7651) in RPMI 1640 (10% fetal bovine serum, 2 mM L-glutamine, 1% penicillin-streptomycin). Cells were permeabilized and stained with antibodies against CD62L (MEL-14), CD4 (GK1), CD45 (30-F11), CD44 (IM7), IL-10 (JES5-16E3), IL-17A (TC11-18H10.1), IL-17F (9D3.1C8), IFN-γ (XMG1.2), and FoxP3 (MK-14) (all BioLegend), preceded by Fc block (BioLegend; #93). Live cells were identified using Live/Dead Fixable Aqua dye (Thermo Fisher Scientific; #L34966A). Samples fixed in 1% PFA were analyzed on a FACSCanto II (BD Biosciences) with FlowJo v10.8.1 (TreeStar). Histological assessments were performed by a blinded pathologist.

Phosphorylation status assessment by proteome profiler antibody array

Phosphorylation profiles of intracellular signaling components following CB_2R modulation were analyzed using the Human Phospho-Kinase Array (R&D Systems, #ARY003C). Jurkat T cells (2.5×10^6 cells/mL) were treated for 10 minutes in supplemented RPMI 1640 containing 1 µM RA ± 1 µM CB_2R agonist JWH-133. Lysates normalized via BCA assay (Thermo Fisher Scientific; #23227) were processed using 300 μg protein per assay membranes (A/B) as per the manufacturer's protocol. Signal intensities were quantified with ImageJ (v1.53; National Institutes of Health).

Assessing intracellular/extracellular target expression via flow cytometry

Jurkat T cells were seeded at 2.5×10^6 cells/mL in RPMI 1640 and treated in triplicate with 1 µM RA ± 1 µM JWH-133 for 48 hours at 37 °C; vehicle control cells received media alone. Following incubation, cells were transferred to V-bottom plates, centrifuged at 1500 *g* for 5 minutes, and resuspended in Hank's Balanced Salt Solution with or without 0.5 mM $MnCl_2$ for integrin activation. For surface staining, cells were incubated with Alexa Fluor 647–conjugated anti-human integrin $\alpha 4\beta 7$ antibody (Bio-Techne/R&D Systems; #FAB10078R) for 30 minutes on ice prior to fixation with 4% PFA at 4 °C. For intracellular staining, the cells were treated for the indicated timepoints, fixed and permeabilized using a commercial buffer set, then stained with Alexa Fluor 647–conjugated anti-human integrin $\alpha 4\beta 7$, APC-conjugated anti-phospho-ERK1/2 (T202/Y204) (Thermo Fisher Scientific, #17-9109-42), PE-conjugated anti-phospho-LCK (Y394) (Bio-Techne/Novus Biologicals; #NBP3-13305), or eFluor 660–conjugated anti-phospho-LCK (Y505) (Thermo Fisher Scientific; #50-9076-42) as appropriate. Live cells were identified using Live/Dead Fixable Aqua dye. Following staining, cells were resuspended in PBS and analyzed on a CytoFLEX LX flow cytometer (Beckman Coulter), with data processed using CytExpert version 2.6 software (Beckman Coulter).

Statistics

Statistical analyses were performed using a 2-tailed T test. Graphs show mean ± SEM and were generated using GraphPad Prism software. Values of $P < .05$ were considered statistically significant.

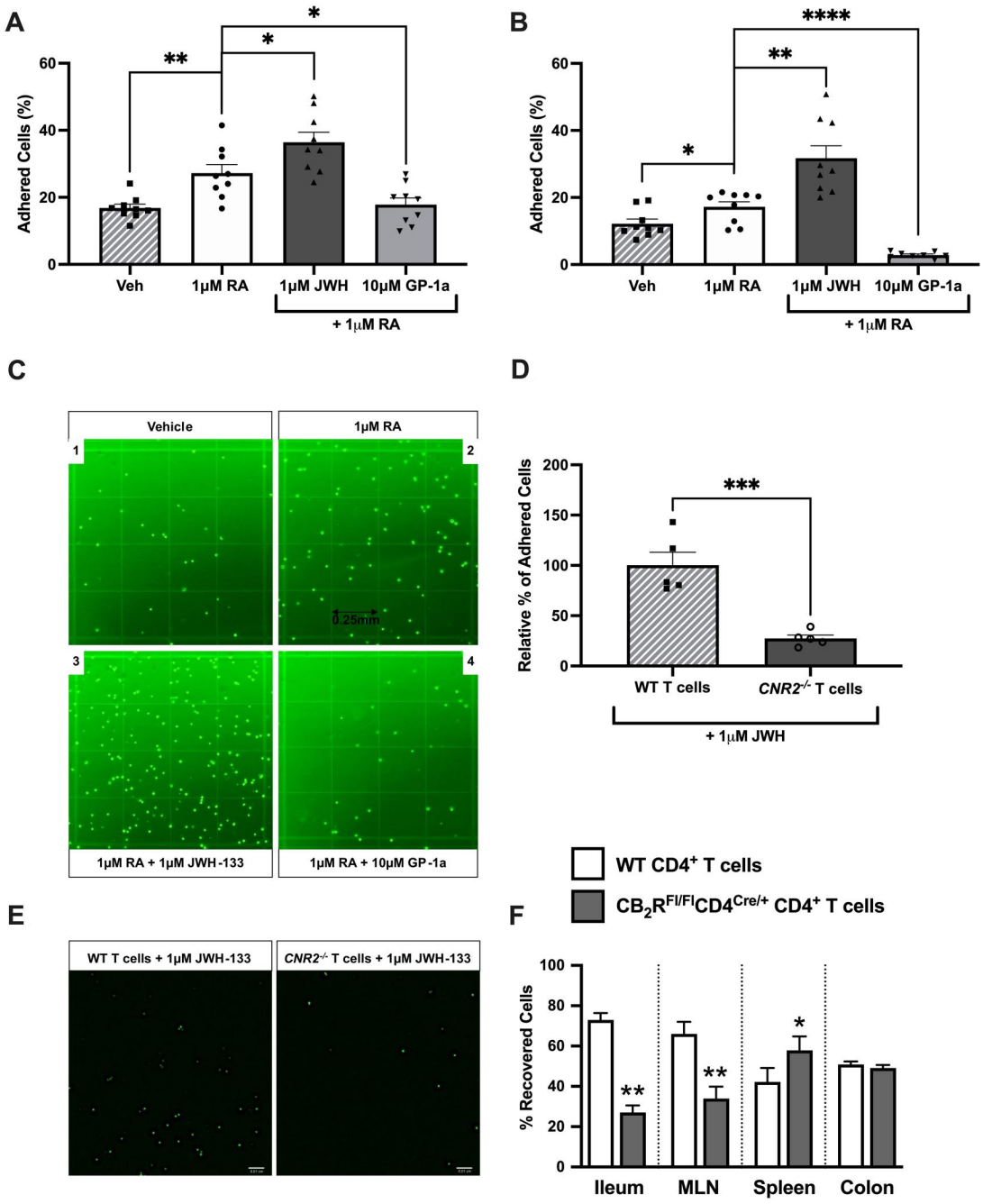

Figure 1 CB_2R signaling induces an increase in integrin $\beta7$ protein expression that functionally binds to mucosal addressin cell adhesion molecule 1 (MAdCAM-1), in a receptor-dependent manner. Static adhesion assays assessing the ability of the CB_2R-mediated $\beta7$ to functionally bind to **(A)** MAdCAM-1–coated plates and **(B,C)** MAdCAM-1–expressing HEK293T cells. **(D,E)** Cellular adhesion assay under shear flow using fluorescently-tagged wild-type (WT) and *CNR2*$^{-/-}$ Jurkat T cells to assess the requirement of CB_2R in inducing the expression of functional $\beta7$ that binds to MAdCAM-1–expressing human umbilical vein endothelial cells (HUVECs).**(F)** In vivo competitive homing assay highlighting a significant decrease in $CD4^+$ T cell frequency in the ileal lamina propria (LP) and mesenteric lymph nodes (MLN) in mice with a T cell-specific deletion of CB_2R, while splenic levels are increased. Results represent mean ± SEM for 3 independent experiments. *$P < .05$, **$P < .01$, ***$P < .001$, ****$P < .0001$. MLN, mesenteric lymph node; RA, retinoic acid.

Results

Increased T cell adherence in response to pharmacological CB_2R activation

To assess whether cannabinoid treatment would make Jurkat T cells more capable of binding to the gut-specific adhesion molecule MAdCAM-1, we used static cellular adhesion assays utilizing MAdCAM-1–coated plates (Figure 1A) and MAdCAM-1–expressing HEK293T cells (Figure 1B, C). RA (1 μM) was also added to induce expression of gut homing integrins on the T cell surface. Consistent with the trend observed at a promoter and transcriptional level, CB_2R inverse agonism with GP-1a (10 μM) significantly reduced the adherence of treated Jurkat T cells to

MAdCAM-1–coated plates and HEK293T endothelial-like cells in both assays. Conversely, CB_2R activation with JWH-133 (1 μM) led to a significant increase in the percentage of adhered cells in both assays following 48 hour cannabinoid treatment. In a more biologically relevant manner, we also assessed the ability of cannabinoid-treated WT and *CNR2*$^{-/-}$ Jurkat T cells to bind to MAdCAM-1–expressing HUVECs under shear flow. Here, the treated T cells were circulated through a fluidics system at a flow rate of 0.4 dyn/cm^3 over a static HUVEC endothelial monolayer, with the percentage of adhered, fluorescently-tagged T cells to the endothelial monolayer being recorded via use of fluorescent confocal microscopy. Consistent with the static assays used, this assay also highlighted the role of CB_2R signaling in mediating functional T cell adhesion. The role of CB_2R activation in inducing the expression of functional $\alpha4\beta7$ and mediating adhesion to MAdCAM-1 was observed to be receptor dependent in this assay, with receptor knockdown mediating a significant decrease in the relative percentage of adhered cells when compared with WT cells (Figure 1D, E). Finally, we examined the contribution of CB_2R to leukocyte trafficking in vivo using a competitive homing assay. Isolated fluorescently labeled $CD4^+$ T cells from WT and $CB_2R^{Fl/Fl}CD4^{Cre+}$ splenocytes were injected intraperitoneally into RAG1$^{-/-}$ lymphopenic hosts and the expression of relative abundance of each genotype was assessed after 24 hours. $CD4^+$ T cells from mice with T cell–specific deletion of CB_2R displayed a significant decrease in frequency in the ileal LP and draining mesenteric lymph node (MLN), while levels of splenic cells were increased. Colonic cell numbers were unaffected which may reflect distinct means of gut homing (Figure 1F). Taken together, these data indicate the role of CB_2R signaling in regulating T cell gut homing both in vitro and in vivo.

CB_2R-mediated regulation of T cell transcription

To better understand how CB_2R signaling might drive an increase in gut homing, we performed bulk RNA sequencing on Jurkat T cells in the presence of the required RA signal. RNA was sequenced from Jurkat T cells treated for 48 hours with RA ± JWH-133 or GP-1a, as well as vehicle-treated control cells, identifying distinct transcriptional profiles of the genes regulated by the two ligands. Respectively, 241 and 142 differentially expressed genes were highlighted following GP-1a or JWH-133 treatment (Figure 2A, B), and a number of these were significantly altered in expression based on their log2 fold change when compared with vehicle-treated cells (Figure 2C, D). These gene sets were obtained via the digital removal of RA-regulated genes, generating two lists made up of genes specifically regulated following CB_2R agonism or inverse agonism (Figure 2E). Using these distinct sets of differentially expressed genes, pathway analysis was used to get a broad view of the specific pathways and gene interaction networks differentially regulated following manipulation of CB_2R signaling. Several pathways pivotal in normal T cell functioning were highlighted, including cellular immune responses and cellular metabolism (Figures S2 and S3), indicating the broad role of the receptor in regulating multiple facets of normal T cell functioning. In the context of the cellular immune response pathways identified, genes such as *CCR4*, *ITGB7*, and *ITGAL* were identified as being some of the top differentially regulated genes (Figure 2C, D), whereas *MYC*, *PIK3R6*, and *HKDC1* were among the top 50 differentially expressed genes following CB_2R manipulation in the context of cellular metabolism, each playing a key role in glucose metabolism specifically. This RNA sequencing data and process of gene set generation was validated using real-time quantitative PCR, with the mRNA expression of several selected candidate genes of interest being shown to mirror the RNA sequencing data in a treatment-specific manner (not shown). Pathway analysis also revealed various in-depth gene-gene interaction networks following receptor agonism or inverse agonism, allowing for a broad view of the potential genetic interactions that may be driving CB_2R-mediated responses in T cells. Taken together, CB_2R signaling drives transcriptional alterations within T cells, with agonist and inverse agonist treatment yielding two distinctly different transcriptional profiles that appear to be important in several normal T cell function including cellular immune responses and glucose metabolism.

CB_2R-mediated regulation of T cell integrin $\beta7$ mRNA and protein expression

Given the impact of CB_2R on driving gut homing and the differential expression of integrin $\beta7$ identified by RNA sequencing, we next examined potential regulation of integrin $\beta7$ by CB_2R at the transcriptional and protein levels. Jurkat T cells were transfected with an integrin $\beta7$ dual luciferase reporter assay to assess $\beta7$ promoter activity in response to cannabinoid treatment in the presence of RA. As previously described, RA alone significantly increased $\beta7$ promoter activity. Following 24 and 48 hour cannabinoid treatment, we observed a significant increase in reporter activity with CB_2R agonism and a corresponding decrease in response to inverse agonism (Figure 3A). Transcriptional regulation of CB_2R signaling on integrin $\beta7$ was also validated using real-time PCR, indicating integrin $\beta7$ mRNA expression to be significantly downregulated and upregulated following CB_2R inverse agonism and agonism, respectively (Figure 3B). In both assays, an earlier time point of 6 hours was also investigated but resulted in no differences among treatment groups (not shown). For scientific rigor and to assess whether the effect of CB_2R signaling on integrin expression was $\beta7$ specific, integrins $\alpha4$, αE, and $\beta1$ mRNA expression levels were also investigated, but no significant alterations in their expression were found across all time points tested (not shown). This indicates that CB_2R signaling regulates integrin expression on T cells in a manner that is selective for integrin $\beta7$.

While interesting to note the role of CB_2R in regulating the expression of integrin $\beta7$ at both the promoter and transcriptional levels, it was also important to assess whether these upstream alterations translated to changes in $\alpha4\beta7$ surface expression at a protein level. This was assessed using flow cytometry. To induce a conformational change in integrin $\alpha4\beta7$ expression towards an activated isoform to allow for effective integrin-antibody binding, the cells were pretreated with $MnCl_2$, which induces a conformational change in integrin presentation facilitating effective antibody binding. Following 48 hour CB_2R agonism, integrin $\beta7$ protein expression was significantly elevated on the surface of T cells, consistent with increased translation of upregulated *ITGB7*

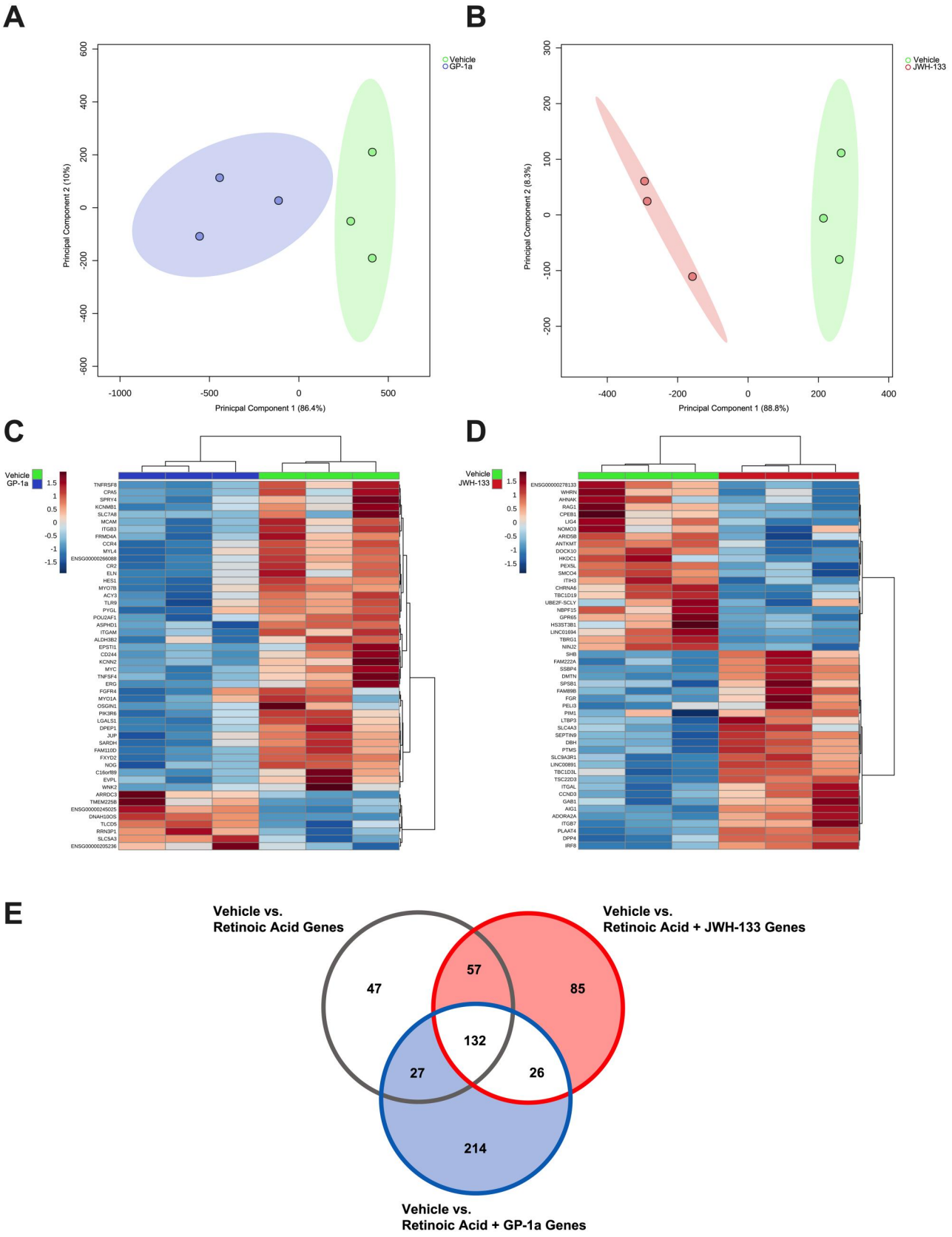

Figure 2 Cannabinoid receptor 2 (CB_2R) drives distinct transcriptional profiles in Jurkat T cells. Bulk RNA sequencing highlighting distinct transcriptional profiles following 48 hour CB_2R modulation (n = 3). Principal component analysis score plots for the genes regulated following treatment with either GP-1a (**A**) or (**B**) JWH-133. $R^2 = 0.903$ and $R^2 = 0.87$, respectively. (**C**, **D**) Heatmaps of the top 50 genes based on Log2FoldChange specifically regulated following CB_2R inverse agonism or agonism, respectively. The degree of expression is indicated by +1.5 (red) and −1.5 (blue). (**E**) Venn diagram of the degree of overlap of differentially expressed genes between treatment groups indicative of the level of change induced by CB_2R signaling.

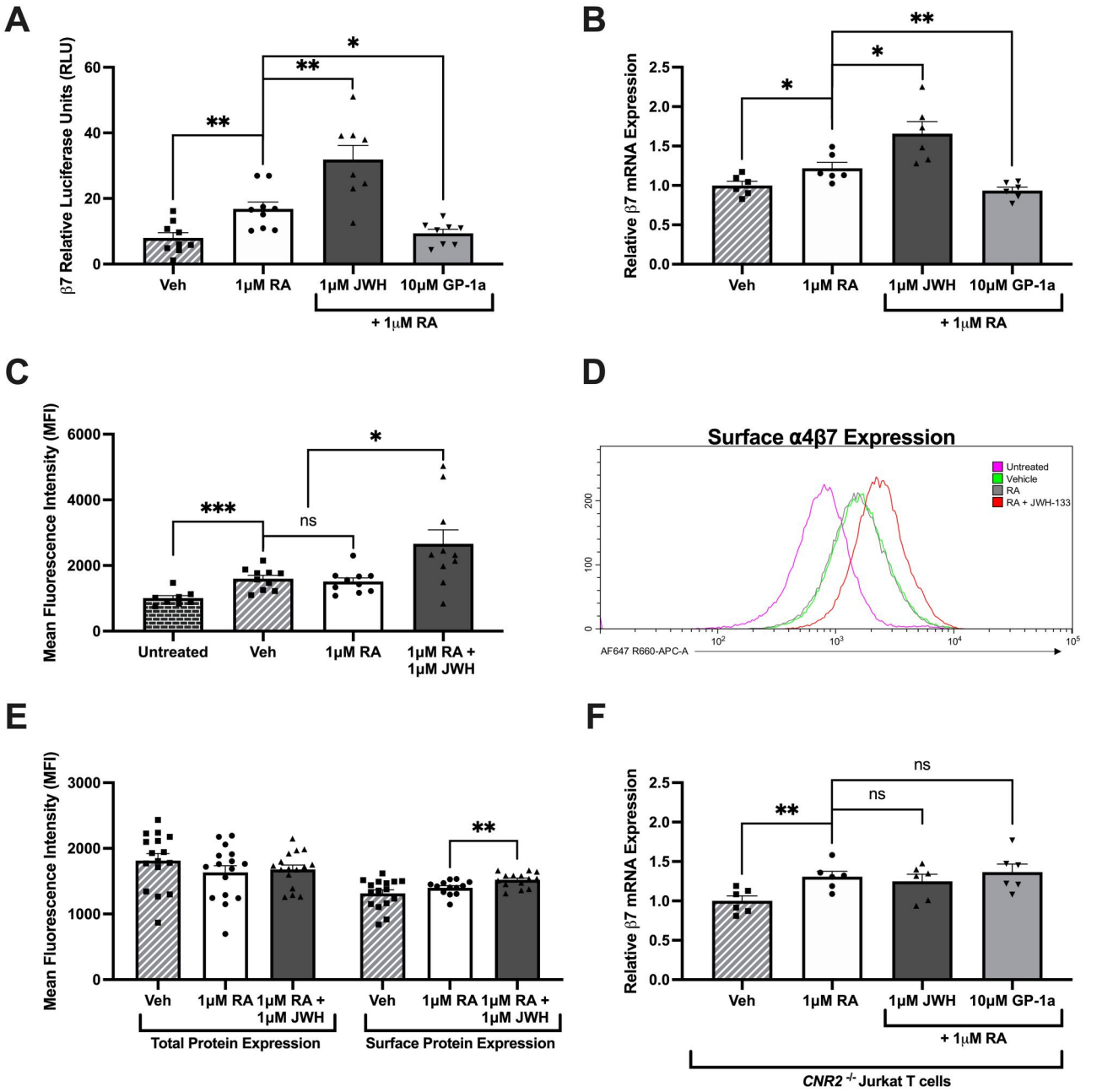

Figure 3 Cannabinoid receptor 2 (CB_2R) activation drives surface expression of integrin $\alpha4\beta7$. **(A)** Integrin $\beta7$ promoter activity assessed using dual luciferase reporter assay after 24 hour cannabinoid treatment in the presence of 1 μM retinoic acid (RA). **(B)** Integrin $\beta7$ messenger RNA (mRNA) expression levels assessed using real-time polymerase chain reaction (PCR) following 24 hour cannabinoid treatment in the presence of 1 μM RA. **(C)** Flow cytometry analysis of integrin expression levels at a surface protein level by means of mean fluorescence intensity (MFI) following 48 hour CB_2R activation in Jurkat T cells. (**D**) Representative histogram overlay of the average MFI values for each treatment group, displaying alterations in surface $\alpha4\beta7$ expression on T cells following CB_2R activation. (**E**) Flow cytometry analysis used to make comparisons between total and surface integrin $\alpha4\beta7$ protein expression levels in Jurkat T cells after 48 hour CB_2R activation. (**F**) Real-time PCR studies investigating integrin $\beta7$ mRNA expression levels in CRISPRi *CNR2*$^{-/-}$ Jurkat T cells following 24 hour cannabinoid treatment. Results represent mean ± SEM for ≥ 3 independent experiments. *$P < .05$, **$P < .01$, ***$P < .001$. ns, not significant; RA, retinoic acid; Veh, vehicle.

mRNA, as indicated by mean fluorescence intensity (MFI) (Figure 3C, D). The requirement for $MnCl_2$ pretreatment was confirmed via flow cytometry analysis without the presence of $MnCl_2$, which failed in facilitating effective integrin-antibody binding and therefore resulted in no changes between any treatment groups at that time point (not shown). We then assessed both the surface $\alpha4\beta7$ protein expression and the whole-cell total $\alpha4\beta7$ protein expression in nonpermeabilized and permeabilized cells, respectively. Interestingly, the elevated expression of $\alpha4\beta7$ following CB_2R activation was induced at a surface protein level, rather than in a total protein manner (Figure 3E).

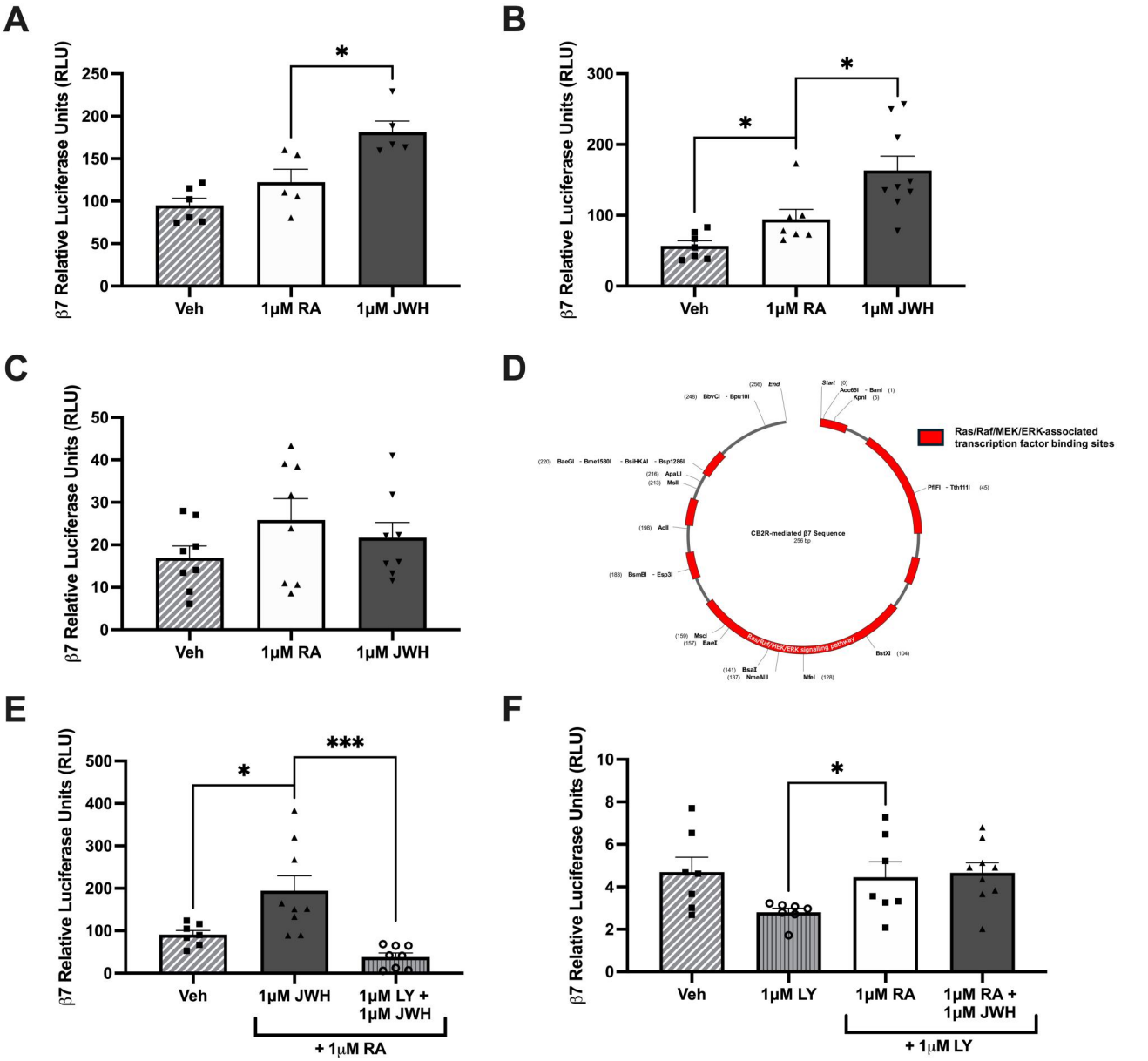

Figure 4 Transcription factor binding site mapping identifies Ras/Raf/MEK/ERK signaling as central to cannabinoid receptor 2 (CB_2R)–mediated $\beta7$ induction. Truncations of the full length $\beta7$ promoter reporter revealed CB_2R induced luciferase activity with **(A)** the full length (FL) plasmid (∼1000 base pairs) and **(B)** truncation 1 (T1) (∼ 750 base pairs) following 24 hour CB_2R activation. In contrast, cells transfected with **(C)** truncation 2 (T2) (∼ 500 base pairs) failed to show any enhancement in integrin $\beta7$ promoter activity relative to retinoic acid (RA)–treated cells following CB_2R activation, indicating the target sequence for CB_2R-mediated $\beta7$ induction to be located within the 250 base pairs between T1 and T2. **(D)** Plasmid map schematic of the specific sequence responsible for CB_2R-mediated $\beta7$ expression in Jurkat T cells. The location of Ras/Raf/MEK/ERK-associated transcription factor binding site locations are displayed in red. Schematic generated using SnapGene and mapped using the Alggen Promo database. **(E)** Dual luciferase reporter assay investigating the Ras/Raf/MEK/ERK-dependent nature of CB_2R-mediated integrin $\beta7$ promoter activity in T cells, using a pan-Raf inhibitor. **(F)** Dual luciferase reporter assay highlighting how Ras/Raf/MEK/ERK inhibition targets the CB_2R-mediated effects on integrin $\beta7$ promoter activity specifically, rather than that of RA. Results represent mean ± SEM for ≥ 3 independent experiments. $^*P < .05$, $^{***}P < .001$. Veh, vehicle.

Following the transfection of a *CNR2* CRISPRi complex under the control of a tetracycline-inducible promoter, we were able to deduce that the significant modulation of integrin $\beta7$ expression in T cells following CB_2R manipulation occurs in a receptor-dependent manner, with those cells with inducible *CNR2* knockdown failing to have any sort of alterations in $\beta7$ expression following 24 hour cannabinoid treatment (Figure 3F). Additionally, *CNR2* knockdown had no effect on RA-induced integrin $\beta7$ expression. Taken together, this data highlights the expansive role of CB_2R signaling in regulating the expression of the gut homing integrin $\beta7$ on T cells at both a promoter and transcriptional level, in a manner that is receptor dependent.

Ras/Raf/MEK/ERK signaling is central to CB_2R-mediated induction of integrin $\beta7$

To explore the mechanism involved in the regulation of CB_2R-mediated integrin $\beta7$ expression on T cells, we used a $\beta7$ promoter truncation assay to aid in identifying the specific sequence responsible for CB_2R-mediated $\beta7$ upregulation. Three $\beta7$ pGL4 plasmid vectors were transfected into Jurkat T cells prior to cannabinoid treatment; full length (FL) (∼1000 base pairs) (Figure 4A), truncation 1 (T1) (∼750 base pairs) (Figure 4B), and truncation 2 (T2) (∼500 base pairs) (Figure 4C). CB_2R activation significantly increased $\beta7$ promoter activity relative to RA-treated samples following 24 hour cannabinoid treatment in those cells transfected with FL and T1. In contrast, those cells transfected with T2 failed to show any enhancement in integrin $\beta7$ promoter activity relative to RA-treated cells following CB_2R activation, indicating the specific sequence for CB_2R-mediated $\beta7$ expression to be located within the 250 base pairs between T1 and T2 (Figure 4C). Using the Alggen Promo database and the FASTA sequence of these 250 base pairs, we were able to map the specific transcription factor binding sites located along the sequence, with Ras/Raf/MEK/ERK pathway–associated transcription factors being the most prominent along the specific sequence (Figure 4D). To further validate whether Ras/Raf/MEK/ERK signaling was involved in the mechanism driving integrin $\beta7$ expression on T cells following CB_2R activation, we utilized the pan-Raf inhibitor LY3009120. Dual luciferase reporter assays found this pan-Raf inhibitor to significantly block the CB_2R-mediated induction in $\beta7$ expression in Jurkat T cells, while having no impact on RA-mediated increases, highlighting the role for this pathway in regulating CB_2R-induced $\beta7$ expression specifically (Figure 4E, F). To summarize, this data reveals the specific genetic sequence responsible for CB_2R-mediated integrin $\beta7$ expression on T cells, something that has not been described previously. Using this sequence, the Raf/Ras/MEK/ERK pathway was found to be central in regulating integrin $\beta7$ expression on T cells following CB_2R activation.

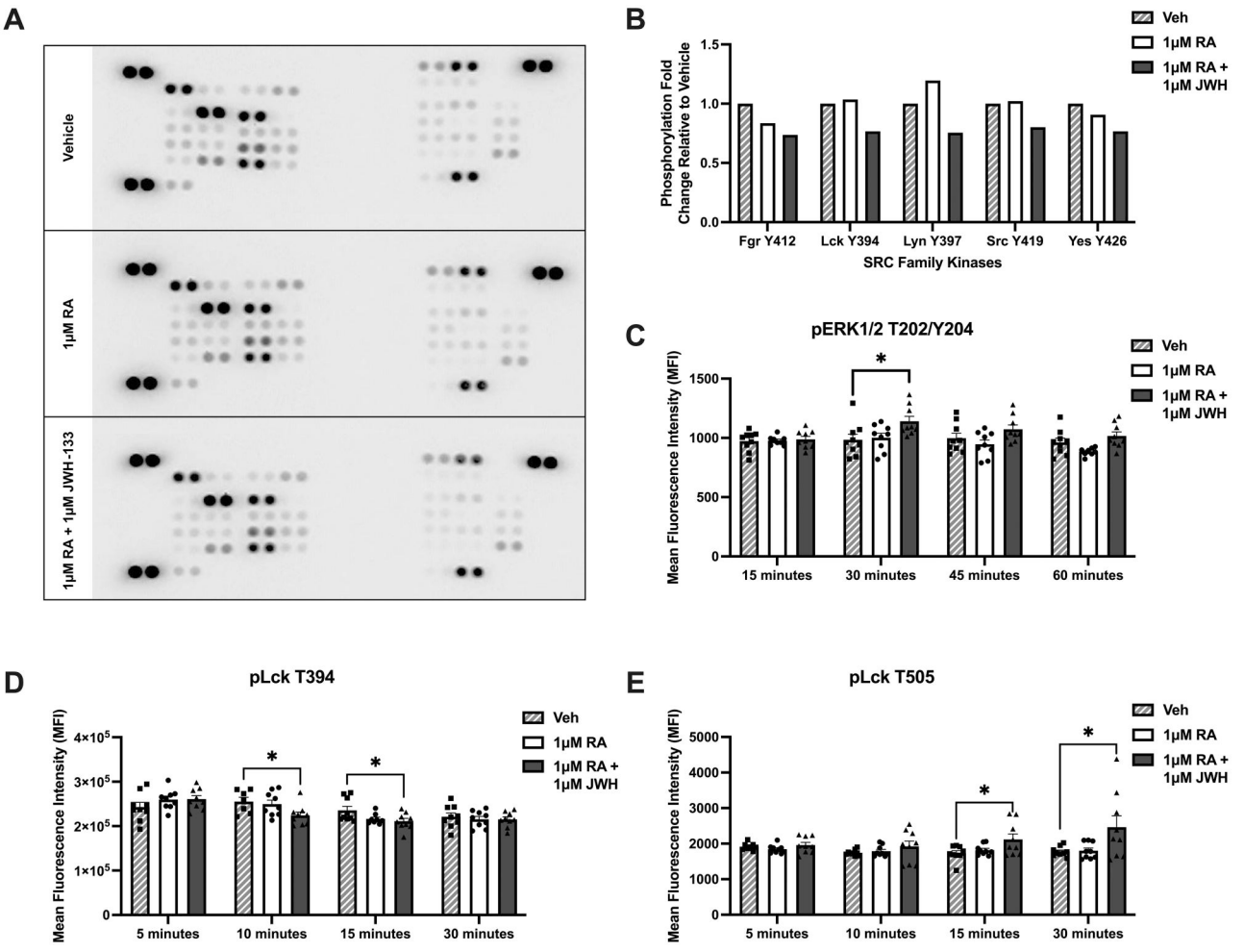

Figure 5 Phosphokinase array identifies potential downstream targets of cannabinoid receptor 2 (CB_2R) that may mediate integrin $\beta7$ expression on T cells following receptor activation. **(A)** Phosphokinase array dot blot following 10 minute CB_2R activation. Dot color intensity is proportional to the degree of protein phosphorylation. **(B)** Densitometry highlighting Src family kinases as being differentially phosphorylated following CB_2R activation. **(C)** Flow cytometry time-course assay assessing the levels of phosphorylated ERK1/2 at the activating site at T202/Y204 in response to CB_2R activation. **(D)** Flow cytometry time-course assay assessing phosphorylated levels of Lck at the activating site T394 following CB_2R activation. **(E)** Flow cytometry time-course assay assessing phosphorylated levels of Lck at the inhibitory site T505 following CB_2R activation. Results represent mean ± SEM for ≥ 3 independent experiments. *$P < .05$. RA, retinoic acid; Veh, vehicle.

Phosphokinase Array identifies downstream targets of CB_2R that may regulate integrin $\beta7$

To assess to what extent ERK1/2 signaling is involved in regulating integrin $\beta7$ expression on T cells following CB_2R activation and to identify potential upstream or downstream regulators, a human phosphokinase dot blot array was used to profile differentially active protein kinases and to investigate the unique kinase network activated following receptor activation in T cells (Figure 5A). Of the 39 proteins tested in the array, members of the Src family of protein tyrosine kinases appeared to be altered following CB_2R activation. These included Fgr, Lck, Lyn, Src, and Yes (Figure 5B). To explore what aspect of the Ras/Raf/MEK/ERK signaling pathway is central in regulating CB_2R-mediated $\beta7$ expression, we focused on ERK signaling due its downstream position in the pathway. A time-course flow cytometry analysis assay assessing the levels of phosphorylated ERK1/2 at the activation site at T202/Y204 following CB_2R activation revealed significant increases in the phosphorylation levels of this protein following 30 minutes of cannabinoid treatment, and subsequent trends toward an increase after 45 and 60 minutes, albeit insignificant (Figure 5C). RA appeared to have no effects on the levels of ERK1/2 phosphorylation at any time point tested, again indicating the CB_2R-specific nature of the involvement of this pathway in regulating integrin $\beta7$ expression on T cells (Figure 5C). To assess the role of Lck in this regard, a time-course flow cytometry analysis assay assessing the levels of phosphorylated Lck at the T394 activation site following CB_2R activation was used. This assay revealed significant decreases in the phosphorylation levels of this kinase after 10 and 15 minutes following CB_2R activation (Figure 5D). Conversely, investigating the phosphorylation levels of Lck at the inhibitory site at T505 found significant increases after 15 and 30 minutes CB_2R activation, further suggesting that Lck signaling is reduced following the activation of CB_2R (Figure 5E). Again, RA treatment appeared to have no significant impact on Lck activity at any of the time points tested. Taken together, these findings suggest the Src family as being potentially important in the ERK signaling responsible for CB_2R-mediated $\alpha4\beta7$ expression on T cells, but in a manner that is independent of Lck kinase activity.

T cell–specific deletion of CB_2R attenuates inflammation in TNF-driven chronic ileitis

Given the ability of CB_2R signaling to promote T cell adherence and upregulation of gut-homing integrin $\beta7$, we next determined if T cell–mediated expression of CB_2R would impact on disease pathogenesis in a chronic preclinical IBD model. Histological examination of inflammatory indices by a trained pathologist (P.J.) blinded to the study identified significant decreases in active inflammation, chronic inflammation, villus distortion, and total inflammatory scores in 20-week-old $TNF^{\Delta ARE/+}CB_2R^{FL/FL}CD4^{Cre/+}$

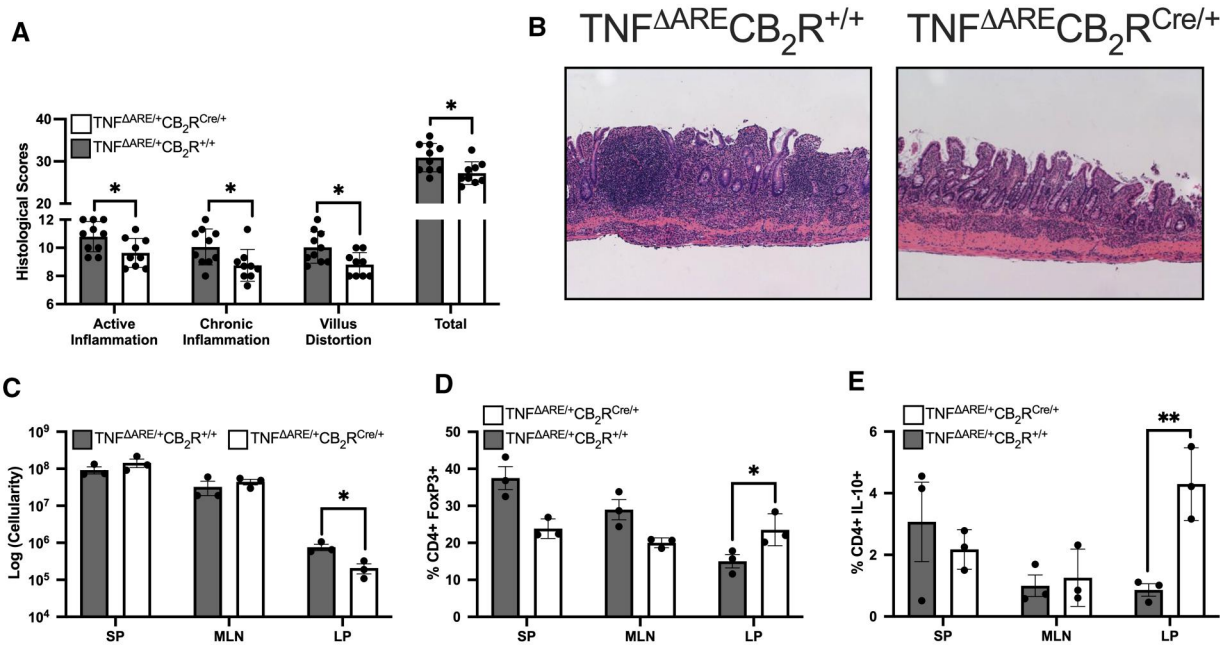

Figure 6 T cell–specific cannabinoid receptor 2 (CB_2R) deletion attenuates chronic murine ileitis in vivo. (**A**) Blinded histological evaluation of intestinal inflammation in the 20-week-old $TNF^{\Delta ARE/+}CB_2R^{Fl/Fl}CD4^{Cre/+}$ ileum of mice with selective deletion of CB_2R from their T cells demonstrated a significant decrease in acute and chronic inflammatory indices in addition to a reduction in villus distortion relative to littermate controls. (**B**) Representative micrographs indicating the improvement in villus architecture and reduction in inflammatory cell infiltrate in $TNF^{\Delta ARE/+}CB_2R^{Fl/Fl}CD4^{Cre/+}$ mice relative to control mice. (**C**) Quantification of lymphocytes recovered from indicated organs support the histological findings of a decrease in cell infiltration into the ileum. Flow cytometry identified a concomitant increase in (**D**) $CD4^+FoxP3^+$ regulatory T cells and (**E**) interleukin-10 producing $CD4^+$ T cells in the ileal lamina propria (LP) of 20-week-old $TNF^{\Delta ARE/+}CB_2R^{Fl/Fl}CD4^{Cre/+}$. Results represent mean ± SEM for 4 to 7 mice per group from ≥ 2 independent experiments. $^*P < .05$, $^{**}P < .01$. MLN, mesenteric lymph node; SP, spleen.

mice compared with littermate control mice (Figure 6A, B). This coincided with a significant decrease in inflammatory cell infiltrate into the ileal LP (Figure 6C). Phenotypic analysis of the T cell subsets within the inflamed gut identified a concomitant increase in relative frequency of $CD4^+$ $FoxP3^+$ regulatory T cells (Figure 6D) as well as $CD4^+$ $IL\text{-}10^+$ anti-inflammatory T cells limited to the ileal LP (Figure 6E). Total numbers of both cell types were unchanged, suggesting that the effect was actually the result of a decrease in inflammatory cells (Figure S4). Taken together, these data support the hypothesis that CB_2R signaling exacerbates intestinal disease driving proinflammatory T cells into the inflamed intestine.

CB_2R deletion coincides with a reduction in central memory T cell expression

To better understand the subsets of T cells that are altered by deletion of CB_2R, we categorized live $CD4^+$ T cells based on expression of CD44 and CD62L, with cells expressing high levels of CD62L and expressing low levels of CD44 referred to as naïve cells, $CD62L^{Low}CD44^{High}$ as effector cells, and $CD62L^{High}CD44^{High}$ cells as central memory T cells (Figure 7A). CB_2R deletion drove a significant decrease in naïve and central memory T cell expression in T cells recovered from the ileal LP (Figure 7B), with those findings echoed in the draining MLN (Figure 7C). Whereas the number of naïve T cells were unaltered in the uninflamed spleen, levels of circulating central memory T cells were also significantly decreased in the spleen (Figure 7D) consistent with findings from the intestinal tissues. Taken together, this points to a decrease in naïve T cell infiltration into the inflamed intestine resulting from a loss of CB_2R signaling, which we attribute to a reduced expression of integrin $\beta 7$. Additionally, T cell–specific deletion of CB_2R appears to also reduce the central memory T cell phenotype, which may be critical to the chronic nature of IBD.

Discussion

The goal of this study was to better understand the contribution of T cell CB_2R signaling to chronic intestinal inflammation. We had previously demonstrated that pharmacological CB_2R inverse agonism with GP-1a attenuated murine ileitis, but an argument could be made that the mechanism reflected the targeting of CB_2R on other cell types.[12] In that study, we demonstrated an increase in endocannabinoid tone in this TNF-driven chronic ileitis model consistent with a role for that system in chronic intestinal disease. We have now taken the process a step further to demonstrate that T cell–specific CB_2R deletion attenuated chronic murine ileitis. This suggests that disrupted CB_2R signaling on T cells alone may be sufficient to induce the previously described anti-inflammatory effect. In that paper, we also demonstrated a role for CB_2R signaling in controlling regulatory T cell suppressive function, a process that is heavily RA dependent.[39] However, RA controls not only regulatory T cell development, but also leukocyte trafficking to the small intestine under both physiological conditions and TNF-driven ileitis.[40,41] When we examined the contribution of CB_2R to leukocyte trafficking in vivo, we demonstrated decreased leukocyte trafficking as a second mechanism whereby CB_2R signaling attenuates ileitis. Attempts to reproduce this in vitro, however, failed unless RA signaling was also included. This led us to test the hypothesis that CB_2R potentiates RA-mediated induction of gut homing $\alpha 4\beta 7$ on T cells, leading to increased $CD4^+$ T cell trafficking to

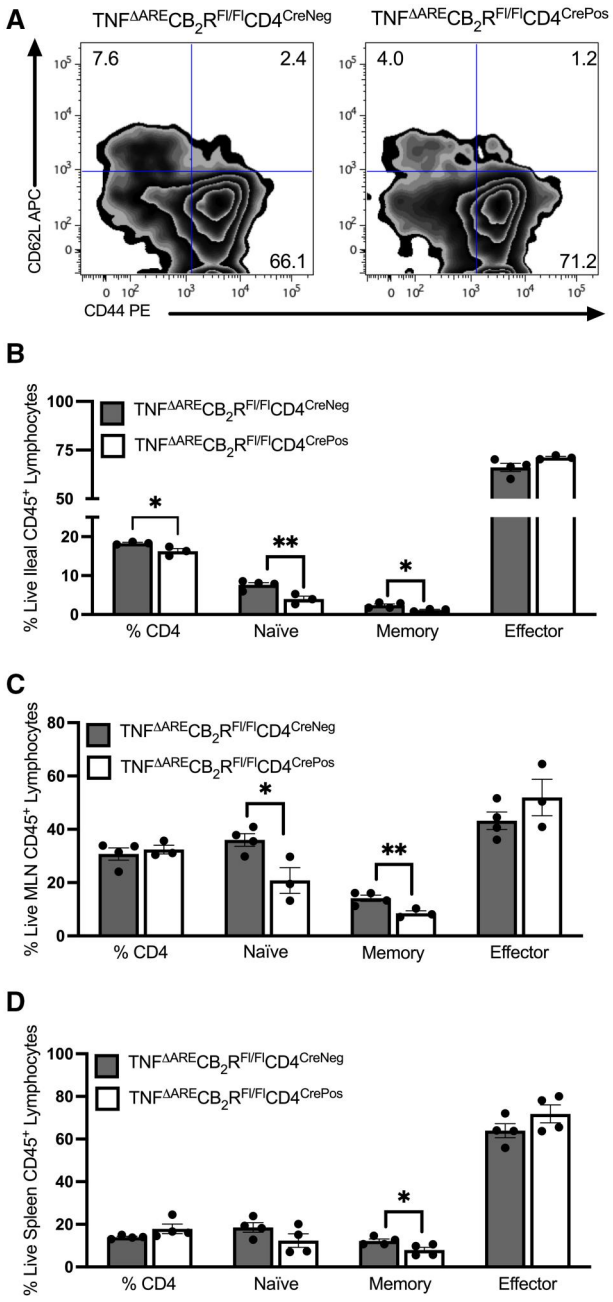

Figure 7 Cannabinoid receptor 2 (CB_2R) deficiency reduces ileal infiltration of naïve and central memory T cells in vivo. (**A**) Representative zebra plots showing flow cytometric analysis of the frequency of live $CD4^+$ T cells expressing CD44 and CD62L from the inflamed ileum lamina propria (LP). Quantification of relative expression of $CD4^+$ T cells, $CD44^{Low}CD62L^{High}$ naïve T cells, $CD44^{High}CD62L^{High}$ central memory T cells, and $CD44^{High}CD62L^{Low}$ effector T cells from the (**B**) ileum, (**C**) mesenteric lymph node (MLN), and (**D**) spleen demonstrate a significant decrease in $CD4^+$ T cells in the ileum only, a decrease in naïve T cell infiltration into both the LP and MLN along with a decrease in memory T cells in all three compartments tested, in 20-week-old $TNF^{\Delta ARE/+}$ mice with selective deletion of CB_2R from their T cells. Results represent mean ± SEM for 4 mice per group from ≥ 2 independent experiments. $^*P < .05$, $^{**}P < .01$.

the small intestine. This increase drives chronic murine ileitis in vivo in a model that is sensitive to disruption of leukocyte trafficking.[41–43] In the presence of RA, CB_2R agonism upregulated integrin $\beta7$ at both message and protein level in both murine and human T cells. Selective CB_2R activation on human leukocytes has also been shown to downregulate active forms of the $\alpha4\beta1$ integrin complex,[44] adding further weight to this hypothesis. While prior studies have linked CB_2R to the regulation of integrins such as $\alpha4\beta1$, $\alpha L\beta2$, and $\alpha M\beta2$, our findings are the first to implicate CB_2R in the modulation of $\alpha4\beta7$ expression.[45,46] Our results indicate that CB_2R activation enhances RA-driven upregulation of $\alpha4\beta7$. This synergistic interaction is consistent with previous reports in other systems, where CB_2R signaling combines with suboptimal RA to promote bone growth and potentiate RAR-mediated transcription in hepatocytes.[47,48] Mapping the sequence conferring CB_2R-dependent regulation of $\beta7$ integrin expression on T cells using truncated promoter-reporters revealed multiple predicted RXR-α binding sites upstream of the $\beta7$ start site. RXR-α, a retinoid X receptor that heterodimerizes with RARs, likely mediates RA signaling at these loci, suggesting direct transcriptional control of $\beta7$ expression by the CB_2R-RA axis.[49] However, *CNR2* knockdown had no effect on RA-induced integrin $\beta7$ expression, indicating that RA does not rely exclusively on CB_2R to mediate $\beta7$ induction. A limitation of this study is that while this offers an implied mechanism for CB_2R to regulate RA signaling, we did not pursue this interaction further. It would be interesting to determine if CB_2R activation alters RAR or RXR receptor phosphorylation, coactivator recruitment, or RA-response element binding in the future. Similarly, the RA for this study was exogenously delivered, rather than derived from $CD103^+$ dendritic cells. While this minimalist design allows for the dissection of T cell–intrinsic mechanism, it is possible that in vivo the effects of CB_2R activation can be overcompensated for with higher local concentrations of RA or RA enhancers such as TGFβ.

The increased $\alpha4\beta7$ expression has functional implications too as demonstrated by adherence assays using immobilized MAdCAM-1 and endothelial monolayers. Once again, CB_2R agonism increased adherence while inverse agonism or receptor knockdown suppressed it. This is in contrast with previous reports of leukocyte CB_2R activation leading to decreased adhesion to brain endothelium and migration across the blood-brain barrier.[45] However, that disparity likely reflects the driving of gut-specific integrin expression instead. Indeed, this effect was so selective that we failed to see alterations in colonic trafficking of CB_2R-deficient T cells likely due to the differential dependence on $\alpha4\beta7$ expression for small and large intestinal trafficking.[50] This has implications for the likely limited applicability of such an approach to treat UC patients or the 30% of people living with Crohn's who do not have small intestinal involvement.

As a G protein–coupled receptor, CB_2R primarily couples to $G_{i/o}$ proteins leading to inhibition of adenylate cyclase, cyclic adenosine monophosphate, and calcium channels.[4] This then triggers activation of MAPKs, including p38, Jun-terminal kinase, ERK1/2, and p44/42 MAPK.[5–7] Transcription factor analysis of the involved promoter sequence revealed a predominance of binding sites for factors downstream of the Ras/Raf/MEK/ERK pathway, notably p53 and c-Jun. Multiple Ras/Raf/MEK/ERK-associated transcription factors were predicted to bind these regulatory regions critical for CB_2R-mediated $\alpha4\beta7$ integrin expression in T cells, further implicating this signaling axis. While Raf/MEK/ERK activation drives integrin $\alpha6$ and $\beta3$ expression, the contribution to integrin $\beta7$ has not been previously described.[51] Using a pan-Raf inhibitor, we were able to confirm the requirement for this pathway in CB_2R-mediated $\alpha4\beta7$ upregulation. To clarify this mechanism, we focused on ERK signaling, as it acts downstream of CB_2R activation and emerged as a key regulator of CB_2R-driven transcriptional responses in T cells during our pathway analysis. Signaling through ERK is also essential for the expression of other integrins such as $\alpha2\beta1$, $\alpha v\beta3$, and $\alpha v\beta5$.[52] RA signaling drives ERK activation in T cells, as evidenced by increased phosphorylation of both ERK1 and ERK2.[53] CB_2R signaling also activates ERK phosphorylation in both neuronal and immune cells.[33,54] Given the established role of ERK signaling in integrin regulation and its activation by both RA and CB_2R pathways, we hypothesized that ERK mediates CB_2R-driven $\alpha4\beta7$ expression in T cells. Using a time-course flow cytometry assay, CB_2R activation significantly increased ERK1/2 phosphorylation at T202/Y204, supporting this hypothesis. These results indicate that indeed the Ras/Raf/MEK/ERK cascade is a key driver of CB_2R-induced $\alpha4\beta7$ expression.

Previous studies indicate that phytocannabinoid treatment promoted $CD4^+$ T cell gut homing in a nonhuman primate simian immunodeficiency virus model.[29] If the same happens in humans, this may go some way to explaining how chronic cannabis use activating CB_2R might lead to worsening disease outcomes for IBD patients.[27] CB_2R expression is upregulated in immune cells across multiple chemically induced colitis models (mustard oil, trinitrobenzene sulfonic acid, dextran sulfate sodium).[14,15] *CNR2* is also significantly upregulated in the inflamed ileum of $TNF^{\Delta ARE}$ mice, with corresponding increases in CB_2R protein levels compared with WT.[12] Elevated CB_2R expression in ileal and colonic biopsy samples from CD and UC patients, respectively, mirrors findings from animal models.[16–18] Numerous studies have also indicated CB_2R to be overexpressed on $CD4^+$T cells isolated from human IBD patients.[15,18,55,56] These studies highlight the potential role of this receptor in IBD progression and intestinal immune regulation.

Antibody blocking $\alpha4\beta7$ with vedolizumab selectively inhibits the intestinal trafficking of $\alpha4\beta7$-expressing T cells, with 41.8% and 39% clinical remissions rate in both UC and CD patients, respectively. Therefore, the finding that CB_2R signaling regulates the expression of $\alpha4\beta7$ on T cells offers therapeutic potential for IBD. Several studies have previously described attenuated colitis following CB_2R activation in murine models in contrast to our findings.[13] Notably, our results align more closely with clinical data from human IBD patients, which show no benefit and, in some cases, worsening outcomes with cannabinoid exposure.[27, 57,58] We propose three potential explanations for this discrepancy. First, the effect may be site-specific, as our adoptive transfers studies saw no difference in T cell trafficking to the colon which might be important for colitis studies, only the ileum which was then reflected in our ileitis model. Second, our model employs chronic ileitis in 20-week-old mice, better mimicking the long-term nature of human IBD compared with the acute chemical colitis studies. Finally, the $TNF^{\Delta ARE/+}$ model, like human disease, is highly T cell dependent, as unfractionated $CD4^+$T cells are sufficient to transfer disease in lymphopenic recipients.[43] Undoubtedly, a limitation of our study is the reliance on this single murine model. While in vivo trafficking studies point to a small intestinal-restricted mechanism, that may only be the case in

the absence of inflammation in RAG recipients. Nonetheless, it would be interesting to determine if T cell–specific CB_2R deficiency equally affected the SAMP1/YitFC or SAMP1 chronic murine ileitis model.[59,60] This model offers benefits, including not only mirroring the polygenic idiopathic nature of CD, but also an opportunity to examine any potential impact on tissue fibrosis and structuring disease. In addition, it would be interesting to see if the impact remains the same in the more epithelial-centric SAMP1/YitFC, in which intestinal barrier disruption precedes intestinal inflammation and oxidative tissue injury, and viscous mucus exudate characterizes the model.[61]

$CD4^+$ T cell–specific CB_2R knockout allows for targeted interrogation of T cell–mediated mechanisms in this model. In contrast, acute colitis models remain disease-prone even in lymphopenic settings consistent with a decreased role for T cells in those models.[62] Nonetheless, GP-1a used in our study has only 30-fold higher affinity for CB_2R over CB_1R, which make it a poor candidate for clinical use.[37] It will be important to examine select ligands with a high degree of specificity for further development.

Together, our findings highlight the need to better understand the molecular mechanisms driving CB_2R-induced immune responses in IBD. We propose that CB_2R may drive leukocyte trafficking into the inflamed intestine and promote a proinflammatory T cell phenotype in CD leading to a worsening flare upon disease reoccurrence. These studies pave the way for future development of novel CB_2R-targeting drugs to broaden the arsenal in the ongoing battle against this incurable lifelong disease. This study also provides mechanistic insight underpinning the known risks associated with cannabis use among people with IBD.

Author contributions

C.B.C. conceived of the study. R.S.L., C.L.H., and H.M.P. conducted experiments, generated reagents, analyzed and interpreted data generated. C.M.A., J.R., and C.J.H. guided the study design, provided reagents, and helped with implementation. G. E. and Z.W. provided guidance in experimental design, equipment, and practical expertise for adherence studies. P.J. provided trained pathology expertise blinded to study design. All authors contributed to refinement of the study protocol and approved the final manuscript.

Supplementary material

Supplementary data is available at *Inflammatory Bowel Diseases* online.

Funding

This work was funded by a Senior Research award from the Crohn's and Colitis Foundation (253596 to C.B.C.) and UCD Ad Astra Fellowship to C.B.C.Additional funding support for $CB_2R^{Fl/Fl}$ mice was provided by the Ministerio de Ciencia e Innovación—Agencia Estatal de Investigación and Fondo Europeo de Desarrollo Regional (Proyecto PID2022-138461OB-I00, supported by MICIU/AEI/10.13039/501100011033 and by FEDER, UE) to J.R.

Conflicts of interest

The authors have declared that no conflict of interest exists.

Data availability

The full analysis dataset is openly available from https://www.ncbi.nlm.nih.gov/bioproject/PRJNA1301825.

References

1. Devlen J, Beusterien K, Yen L, Ahmed A, Cheifetz AS, Moss AC. The burden of inflammatory bowel disease: a patient-reported qualitative analysis and development of a conceptual model. *Inflamm Bowel Dis*. 2014;20:545-552. https://doi.org/10.1097/01.MIB.0000440983.86659.81
2. Schirbel A, Reichert A, Roll S, et al. Impact of pain on health-related quality of life in patients with inflammatory bowel disease. *World J Gastroenterol*. 2010;16:3168-3177. https://doi.org/10.3748/wjg.v16.i25.3168
3. Lala A, Rodriguez-Palacios A, Cominelli F, Basson AR. Inflammatory bowel disease patients believe cannabis and cannabidiol oil relieve symptoms. *Acad Med (San Franc)*. 2025;2(2). https://doi.org/10.20935/acadmed7773
4. Glass M, Northup JK. Agonist selective regulation of G proteins by cannabinoid CB1 and CB2 receptors. *Mol Pharmacol*. 1999;56:1362-1369. https://doi.org/10.1016/S0026-895X(24)12404-2
5. Almogi-Hazan O, Or R. Cannabis, the endocannabinoid system and immunity-the journey from the bedside to the bench and back. *Int J Mol Sci*. 2020;21:4448. https://doi.org/10.3390/ijms21124448
6. Pacher P, Bátkai S, Kunos G. The endocannabinoid system as an emerging target of pharmacotherapy. *Pharmacol Rev*. 2006;58:389-462. https://doi.org/10.1124/pr.58.3.2
7. Perisetti A, Rimu AH, Khan SA, Bansal P, Goyal H. Role of cannabis in inflammatory bowel diseases. *Ann Gastroenterol*. 2020;33:134-144. https://doi.org/10.20524/aog.2020.0452
8. Rodriguez de Fonseca F, Del Arco I, Bermudez-Silva FJ, Bilbao A, Cippitelli A, Navarro M. The endocannabinoid system: physiology and pharmacology. *Alcohol and Alcoholism*. 2005;40:2-14. https://doi.org/10.1093/alcalc/agh110
9. Percie Du Sert N, Ho WSV, Rudd JA, Andrews PLR. Cannabinoid-induced reduction in antral pacemaker frequency: a telemetric study in the ferret: cannabinoids and gastric myoelectric activity. *Neurogastroenterol Motil*. 2010;22:1257-1266, e324. https://doi.org/10.1111/j.1365-2982.2010.01581.x
10. Martinez Ramirez CE, Ruiz-Pérez G, Stollenwerk TM, Behlke C, Doherty A, Hillard CJ. Endocannabinoid signaling in the central nervous system. *Glia*. 2023;71:5-35. https://doi.org/10.1002/glia.24280
11. Ruiz de Martín Esteban S, Benito-Cuesta I, Terradillos I, et al. Cannabinoid CB(2) receptors modulate microglia function and amyloid dynamics in a mouse model of Alzheimer's disease. *Front Pharmacol*. 2022;13:841766. https://doi.org/10.3389/fphar.2022.841766
12. Leinwand KL, Jones AA, Huang RH, et al. Cannabinoid receptor-2 ameliorates inflammation in murine model of

Crohn's disease. *J Crohns Colitis*. 2017;11:1369-1380. https://doi.org/10.1093/ec1jcc/jjx096
13. Leinwand KL, Gerich ME, Hoffenberg EJ, Collins CB. Manipulation of the endocannabinoid system in colitis: a comprehensive review. *Inflamm Bowel Dis*. 2017;23:192-199. https://doi.org/10.1097/MIB.0000000000001004
14. Kimball ES, Schneider CR, Wallace NH, Hornby PJ. Agonists of cannabinoid receptor 1 and 2 inhibit experimental colitis induced by oil of mustard and by dextran sulfate sodium. *Am J Physiol Gastrointest Liver Physiol*. 2006;291:G364-G371. https://doi.org/10.1152/ajpgi.00407.2005
15. Storr MA, Keenan CM, Zhang H, Patel KD, Makriyannis A, Sharkey KA. Activation of the cannabinoid 2 receptor (CB2) protects against experimental colitis. *Inflamm Bowel Dis*. 2009;15:1678-1685. https://doi.org/10.1002/ibd.20960
16. Marquéz L, Suárez J, Iglesias M, Bermudez-Silva FJ, de Fonseca FR, Andreu M. Ulcerative colitis induces changes on the expression of the endocannabinoid system in the human colonic tissue. *PLoS One*. 2009;4:e6893. https://doi.org/10.1371/journal.pone.0006893.
17. Stintzing S, Wissniowski TT, Lohwasser C, Alinger B, Neureiter D, Ocker M. Role of cannabinoid receptors and RAGE in inflammatory bowel disease. *Histol Histopathol*. 2011;26:735-745. https://doi.org/10.14670/HH-26.735
18. Strisciuglio C, Creoli M, Tortora C, et al. Increased expression of CB2 receptor in the intestinal biopsies of children with inflammatory bowel disease. *Pediatr Res*. 2023;93:520-525. https://doi.org/10.1038/s41390-022-02109-5
19. D'Argenio G, Valenti M, Scaglione G, Cosenza V, Sorrentini I, Di Marzo V. Up-regulation of anandamide levels as an endogenous mechanism and a pharmacological strategy to limit colon inflammation. *FASEB J*. 2006;20:568-570. https://doi.org/10.1096/fj.05-4943fje
20. Darmani NA, Izzo AA, Degenhardt B, et al. Involvement of the cannabimimetic compound, N-palmitoyl-ethanolamine, in inflammatory and neuropathic conditions: review of the available pre-clinical data, and first human studies. *Neuropharmacology*. 2005;48:1154-1163. https://doi.org/10.1016/j.neuropharm.2005.01.001
21. Klein TW, Cabral GA. Cannabinoid-induced immune suppression and modulation of antigen-presenting cells. *J Neuroimmune Pharmacol*. 2006;1:50-64. https://doi.org/10.1007/s11481-005-9007-x
22. Castro J, Garcia-Caraballo S, Maddern J, et al. Olorinab (APD371), a peripherally acting, highly selective, full agonist of the cannabinoid receptor 2, reduces colitis-induced acute and chronic visceral hypersensitivity in rodents. *Pain*. 2022;163:e72-e86. https://doi.org/10.1097/j.pain.0000000000002314
23. Naftali T, Bar-Lev Schleider L, Dotan I, Lansky EP, Sklerovsky Benjaminov F, Konikoff FM. Cannabis induces a clinical response in patients with Crohn's disease: a prospective placebo-controlled study. *Clin Gastroenterol Hepatol*. 2013;11:1276-1280.e1. https://doi.org/10.1016/j.cgh.2013.04.034
24. Irving PM, Iqbal T, Nwokolo C, et al. A randomized, double-blind, placebo-controlled, parallel-group, pilot study of cannabidiol-rich botanical extract in the symptomatic treatment of ulcerative colitis. *Inflamm Bowel Dis*. 2018;24:714-724. https://doi.org/10.1093/ibd/izy002
25. Naftali T, Schleider LB-L, Benjaminov FS, Konikoff FM, Matalon ST, Ringel Y. Cannabis is associated with clinical but not endoscopic remission in ulcerative colitis: a randomized controlled trial. *PLoS One*. 2021;16:e0246871. https://doi.org/10.1371/journal.pone.0246871
26. Volz MS, Siegmund B, Häuser W. Efficacy, tolerability, and safety of cannabinoids in gastroenterology: a systematic review. *Schmerz*. 2016;30:37-46. https://doi.org/10.1007/s00482-015-0087-0
27. Storr M, Devlin S, Kaplan GG, Panaccione R, Andrews CN. Cannabis use provides symptom relief in patients with inflammatory bowel disease but is associated with worse disease prognosis in patients with Crohn's disease. *Inflamm Bowel Dis*. 2014;20:472-480. https://doi.org/10.1097/01.MIB.0000440982.79036.d6
28. Palazuelos J, Davoust N, Julien B, et al. The CB2 cannabinoid receptor controls myeloid progenitor trafficking: involvement in the pathogenesis of an animal model of multiple sclerosis. *J Biol Chem*. 2008;283:13320-13329. https://doi.org/10.1074/jbc.M707960200
29. Molina PE, Amedee AM, LeCapitaine NJ, et al. Modulation of Gut-specific mechanisms by chronic Δ9-Tetrahydrocannabinol administration in male rhesus macaques infected with simian immunodeficiency virus: a systems biology analysis. *AIDS Res Hum Retroviruses*. 2014;30:567-578. https://doi.org/10.1089/aid.2013.0182
30. Hamann A, Andrew DP, Jablonski-Westrich D, Holzmann B, Butcher EC. Role of alpha 4-integrins in lymphocyte homing to mucosal tissues in vivo. *J Immunol*. 1994;152:3282-3293. https://doi.org/10.4049/jimmunol.152.7.3282
31. Szilagyi BA, Triebus J, Kressler C, et al. Gut memories do not fade: epigenetic regulation of lasting gut homing receptor expression in CD4+ memory T cells. *Mucosal Immunol*. 2017;10:1443-1454. https://doi.org/10.1038/mi.2017.7
32. Di Giacomo D, De Domenico E, Sette C, Geremia R, Grimaldi P. Type 2 cannabinoid receptor contributes to the physiological regulation of spermatogenesis. *Faseb J*. 2016;30:1453-1463. https://doi.org/10.1096/fj.15-279034
33. Bouaboula M, Poinot-Chazel C, Marchand J, et al. Signaling pathway associated with stimulation of CB2 peripheral cannabinoid receptor: involvement of both mitogen-activated protein kinase and induction of Krox-24 expression. *Eur J Biochem*. 1996;237:704-711. https://doi.org/10.1111/j.1432-1033.1996.0704p.x
34. Basu S, Ray A, Dittel BN. Cannabinoid receptor 2 is critical for the homing and retention of marginal zone B lineage cells and for efficient T-independent immune responses. *J Immunol*. 2011;187:5720-5732. https://doi.org/10.4049/jimmunol.1102195
35. Wang J, Xu J, Liu J, et al. Genetic variant Q63R of cannabinoid receptor 2 causes differential ERK phosphorylation in human immune cells. *Genet Test Mol Biomarkers*. 2018;22:320-326. https://doi.org/10.1089/gtmb.2018.0005
36. Hytti M, Andjelic S, Josifovska N, et al. CB2 receptor activation causes an ERK1/2-dependent inflammatory response in human RPE cells. *Sci Rep*. 2017;7:16169. https://doi.org/10.1038/s41598-017-16524-w
37. Soethoudt M, Grether U, Fingerle J, et al. Cannabinoid CB(2) receptor ligand profiling reveals biased signalling and off-

target activity. *Nat Commun*. 2017;8:13958. https://doi.org/10.1038/ncomms13958
38. López A, Aparicio N, Pazos MR, et al. Cannabinoid CB(2) receptors in the mouse brain: relevance for Alzheimer's disease. *J Neuroinflammation*. 2018;15:158. https://doi.org/10.1186/s12974-018-1174-9
39. Iwata M, Hirakiyama A, Eshima Y, Kagechika H, Kato C, Song SY. Retinoic acid imprints gut-homing specificity on T cells. *Immunity*. 2004;21:527-538. https://doi.org/10.1016/j.immuni.2004.08.011
40. Sun C-M, Hall JA, Blank RB, et al. Small intestine lamina propria dendritic cells promote de novo generation of Foxp3 T reg cells via retinoic acid. *J Exp Med*. 2007;204:1775-1785. https://doi.org/10.1084/jem.20070602
41. Collins CB, Aherne CM, Kominsky D, et al. Retinoic acid attenuates ileitis by restoring the balance between T-helper 17 and T regulatory cells. *Gastroenterology*. 2011;141:1821-1831. https://doi.org/10.1053/j.gastro.2011.05.049
42. Collins CB, Aherne CM, McNamee EN, et al. Flt3 ligand expands CD103(+) dendritic cells and FoxP3(+) T regulatory cells, and attenuates Crohn's-like murine ileitis. *Gut*. 2012;61:1154-1162. https://doi.org/10.1136/gutjnl-2011-300820
43. Collins CB, Ho J, Wilson TE, et al. CD44 deficiency attenuates chronic murine ileitis. *Gastroenterology*. 2008;135:1993-2002. https://doi.org/10.1053/j.gastro.2008.08.053
44. Pereira JP, An J, Xu Y, Huang Y, Cyster JG. Cannabinoid receptor 2 mediates the retention of immature B cells in bone marrow sinusoids. *Nat Immunol*. 2009;10:403-411. https://doi.org/10.1038/ni.1710
45. Rom S, Zuluaga-Ramirez V, Dykstra H, Reichenbach NL, Pacher P, Persidsky Y. Selective activation of cannabinoid receptor 2 in leukocytes suppresses their engagement of the brain endothelium and protects the blood-brain barrier. *Am J Pathol*. 2013;183:1548-1558. https://doi.org/10.1016/j.ajpath.2013.07.033
46. Montecucco F, Lenglet S, Braunersreuther V, et al. CB2 cannabinoid receptor activation is cardioprotective in a mouse model of ischemia/reperfusion. *J Mol Cell Cardiol*. 2009;46:612-620. https://doi.org/10.1016/j.yjmcc.2008.12.014
47. Haspula D, Clark MA. Cannabinoid receptors: an update on cell signaling, pathophysiological roles and therapeutic opportunities in neurological, cardiovascular, and inflammatory diseases. *Int J Mol Sci*. 2020;21:7693. https://doi.org/10.3390/ijms21207693
48. Fraher D, Mann RJ, Dubuisson MJ, et al. The endocannabinoid system and retinoic acid signaling combine to influence bone growth. *Mol Cell Endocrinol*. 2021;529:111267. https://doi.org/10.1016/j.mce.2021.111267
49. Delmotte MH, Tahayato A, Formstecher P, Lefebvre P. Serine 157, a retinoic acid receptor α residue phosphorylated by protein kinase C in vitro, is involved in RXR· RARα heterodimerization and transcriptional activity. *J Biol Chem*. 1999;274:38225-38231. https://doi.org/10.1074/jbc.274.53.38225
50. Dzutsev A, Hogg A, Sui Y, et al. Differential T cell homing to colon vs. small intestine is imprinted by local CD11c(+) APCs that determine homing receptors. *J Leukoc Biol*. 2017;102:1381-1388. https://doi.org/10.1189/jlb.1A1116-463RR
51. Woods D, Cherwinski H, Venetsanakos E, et al. Induction of β3-integrin gene expression by sustained activation of the Ras-regulated Raf–MEK–extracellular signal-regulated kinase signaling pathway. *Mol Cell Biol*. 2001;21:3192-3205. https://doi.org/10.1128/MCB.21.9.3192-3205.2001
52. Lai CF, Chaudhary L, Fausto A, et al. Erk is essential for growth, differentiation, integrin expression, and cell function in human osteoblastic cells. *J Biol Chem*. 2001;276:14443-14450. https://doi.org/10.1074/jbc.M010021200
53. Wu S, Wang W, Le Q. All-trans retinoic acid regulates the balance of Treg-Th17 cells through ERK and P38 signaling pathway. *Iran J Immunol*. 2019;16:1-10. https://doi.org/10.22034/IJI.2019.39402
54. Basu S, Dittel BN. Unraveling the complexities of cannabinoid receptor 2 (CB2) immune regulation in health and disease. *Immunol Res*. 2011;51:26-38. https://doi.org/10.1007/s12026-011-8210-5
55. Wright K, Rooney N, Feeney M, et al. Differential expression of cannabinoid receptors in the human colon: cannabinoids promote epithelial wound healing. *Gastroenterology*. 2005;129:437-453. https://doi.org/10.1016/j.gastro.2005.05.026
56. Hryhorowicz S, Kaczmarek-Ryś M, Zielińska A, Scott RJ, Słomski R, Pławski A. Endocannabinoid system as a promising therapeutic target in inflammatory bowel disease–a systematic review. *Front Immunol*. 2021;12:790803. https://doi.org/10.3389/fimmu.2021.790803
57. Naftali T, Lev LB, Yablecovitch D, Yablekovitz D, Half E, Konikoff FM. Treatment of Crohn's disease with cannabis: an observational study. *Isr Med Assoc J*. 2011;13:455-458.
58. Naftali T, Mechulam R, Marii A, et al. Low-dose cannabidiol is safe but not effective in the treatment for Crohn's disease, a randomized controlled trial. *Dig Dis Sci*. 2017;62:1615-1620. https://doi.org/10.1007/s10620-017-4540-z
59. Pizarro TT, Pastorelli L, Bamias G, et al. SAMP1/YitFc mouse strain: a spontaneous model of Crohn's disease-like ileitis. *Inflamm Bowel Dis*. 2011;17:2566-2584. https://doi.org/10.1002/ibd.21638
60. McNamee EN, Wermers JD, Masterson JC, et al. Novel model of TH2-polarized chronic ileitis: the SAMP1 mouse. *Inflamm Bowel Dis*. 2010;16:743-752. https://doi.org/10.1002/ibd.21148
61. Drieu La Rochelle J, Ward J, Stenke E, et al. Dysregulated NOX1-NOS2 activity as hallmark of ileitis in mice. *Mucosal Immunol*. 2024;17:1326-1336. https://doi.org/10.1016/j.mucimm.2024.08.012
62. Katakura K, Lee J, Rachmilewitz D, Li G, Eckmann L, Raz E. Toll-like receptor 9-induced type I IFN protects mice from experimental colitis. *J Clin Invest*. 2005;115:695-702. https://doi.org/10.1172/JCI22996